Neuron, Vol. 36, 635–648, November 14, 2002, Copyright ©2002 by Cell Press

Roles of Neurotransmitter in Synapse Formation: Development of Neuromuscular Junctions Lacking Choline Acetyltransferase

Thomas Misgeld, Robert W. Burgess, Renate M. Lewis, Jeanette M. Cunningham, Jeff W. Lichtman,[1] and Joshua R. Sanes[1]
Department of Anatomy and Neurobiology
Washington University School of Medicine
St. Louis, Missouri 63110

Summary

Activity-dependent and -independent signals collaborate to regulate synaptogenesis, but their relative contributions are unclear. Here, we describe the formation of neuromuscular synapses at which neurotransmission is completely and specifically blocked by mutation of the neurotransmitter-synthesizing enzyme choline acetyltransferase. Nerve terminals differentiate extensively in the absence of neurotransmitter, but neurotransmission plays multiple roles in synaptic differentiation. These include influences on the numbers of pre- and postsynaptic partners, the distribution of synapses in the target field, the number of synaptic sites per target cell, and the number of axons per synaptic site. Neurotransmission also regulates the formation or stability of transient acetylcholine receptor-rich processes (myopodia) that may initiate nerve-muscle contact. At subsequent stages, neurotransmission delays some steps in synaptic maturation but accelerates others. Thus, neurotransmission affects synaptogenesis from early stages and coordinates rather than drives synaptic maturation.

Introduction

Synaptogenesis is directed by a combination of activity-independent molecular cues that specify neural connections and activity-dependent epigenetic factors that permit experience to shape them. One widely accepted view is that the earliest events in synaptic differentiation can occur in the absence of either pre- or postsynaptic activity, whereas later steps depend on synaptic transmission and/or the electrical responses that transmission evokes (reviewed in Goodman and Shatz, 1993; Zhang and Poo, 2001). However, it has been difficult to test this model in vivo for several reasons. First, most methods for inhibiting neurotransmission in vertebrates have, until recently, involved pharmacological interventions that imposed blockade after synaptogenesis was already underway or terminated it before synapses had fully developed (e.g., Harris, 1981b; Duxson, 1982; Oppenheim et al., 1989; Houenou et al., 1990; Dahm and Landmesser, 1991). Second, in some cases, perturbations meant to inhibit neurotransmitter release do so incompletely, blocking evoked but not spontaneous release (e.g., Harris, 1981b; Houenou et al., 1990; Broadie and Bate, 1993; Deitcher et al., 1998; Washbourne et al., 2002). Likewise, blockade of postsynaptic receptors (e.g., Gordon et al., 1974; Betz et al., 1980; Duxson, 1982; Oppenheim et al., 1989; Dahm and Landmesser, 1991; Ding et al., 1983; Sepich et al., 1998) is often incomplete. These are serious concerns, in that even low, spontaneous levels of neurotransmitter release may affect postsynaptic receptor number and distribution (Akaaboune et al., 1999; Saitoe et al., 2001; but see Featherstone et al., 2002; Varoqueaux et al., 2002). Thus, processes that appear to be activity independent may actually require spontaneous activity. Third, some manipulations that block synaptic transmission deprive the postsynaptic cell of more than synaptic currents. For example, blocking exocytosis from nerve terminals (Sweeney et al., 1995; Verhage et al., 2000) may prevent release of trophic factors or synaptic organizing molecules as well as neurotransmitter. Thus, processes believed to require postsynaptic excitation may instead depend on secretion of signaling molecules from the nerve. Finally, genetic manipulations that disrupt synaptogenesis by blocking delivery or effects of molecular cues (e.g., Gautam et al., 1995, 1996; DeChiara et al., 1996) of necessity perturb synaptic transmission, so some effects attributed to the activity-independent signaling pathway may be secondary consequences of inactivity.

Here, to circumvent these limitations, we analyzed the formation of neuromuscular junctions (NMJs) in mutant mice lacking the acetylcholine-synthesizing enzyme choline acetyltransferase (ChAT). We believe that this mutation provides the best currently available means for selectively blocking neurotransmission in vivo. First, acetylcholine underlies both evoked and spontaneous synaptic activity at all vertebrate NMJs. Second, there is only a single *ChAT* gene in the mammalian genome. Third, neurotransmission is the only established function for acetylcholine in the nervous system. Fourth, cholinergic synaptic vesicles form and undergo exocytosis even when depleted of acetylcholine (Parsons et al., 1999). Thus, we reasoned that NMJs in mice lacking ChAT would not undergo aspects of synaptogenesis that require neurotransmitter or neurotransmission but would still undergo those that are neurotransmitter independent. Analysis of these mice revealed a remarkable array of both pre- and postsynaptic abnormalities even at early stages of synapse formation. At later stages, some aspects of synaptic maturation were delayed, but others occurred sooner in mutants than in controls. Our results require revision of the views that initial aspects of synaptogenesis are activity independent and that neurotransmission simply promotes synaptic maturation.

Results

Targeted Deletion of ChAT Abolishes Neurotransmission at the NMJ

To inactivate the *ChAT* gene in mice, we used cre-mediated excision to replace exons 3 and 4 with the gene for neomycin phosphoryltransferase (Figures 1A and 1B;

[1]Correspondence: sanesj@pcg.wustl.edu (J.R.S.), jeff@pcg.wustl.edu (J.W.L.)

see Experimental Procedures for details). *ChAT*$^{+/-}$ mice appeared normal, and *ChAT*$^{-/-}$ embryos were viable until late gestational stages (29−/−, 58+/−, and 35+/+ pups in 13 genotyped litters at E17–18, corresponding to Mendelian frequency at $p > 0.6$ by χ^2 test). However, *ChAT*$^{-/-}$ pups died at birth, were never seen to move, and showed postural abnormalities characteristic of flaccid paralysis, such as a hunched back (Figure 1C) and palmar flexion of the front paws. These abnormalities almost certainly result from the neuromuscular defects described below.

To confirm that the mutation had eliminated ChAT and neuromuscular transmission, we first amplified mRNA produced from the mutant allele by RT-PCR, using primers in exons 2 plus either exon 8 or exon 15 (Figure 1D and data not shown). Sequencing of products revealed that all resulted from splicing of exon 2 to exon 5, resulting in a frame shift after the codon for amino acid 22 and a stop codon nine amino acids later. Thus, while truncated transcripts were produced from the mutant allele, all encoded protein products were <32 amino acids long (instead of 641) and lacked the enzyme's catalytic center (Carbini and Hersh, 1993). Second, we used immunohistochemistry to seek residual ChAT in spinal cord. ChAT immunoreactivity was demonstrable in wild-type motoneurons but not in motoneurons from *ChAT*$^{-/-}$ embryos (Figure 1E). Third, we tested the possibility that an enzyme other than ChAT was capable of acetylating choline to generate acetylcholine in mutants. Choline acetylating activity was present in lysates prepared from brains of wild-type mice but not in those from *ChAT*$^{-/-}$ mutants (Figure 1F). Finally, we recorded intracellularly from myotubes to test the possibility that another neurotransmitter was capable of eliciting postsynaptic responses. Stimulation of motor nerves evoked excitatory postsynaptic potentials from control myotubes (6/6) but not from mutant myotubes (0/11), even after increasing stimulus intensity or duration severalfold (Figure 1G; note larger stimulus artifact in mutant than control). Likewise stimulation elicited visible contractions in muscles from controls (16/16 muscles tested) but not mutants (0/10), even though direct electrical stimulation of mutant muscle elicited vigorous contractions, showing that myotubes were electrically excitable.

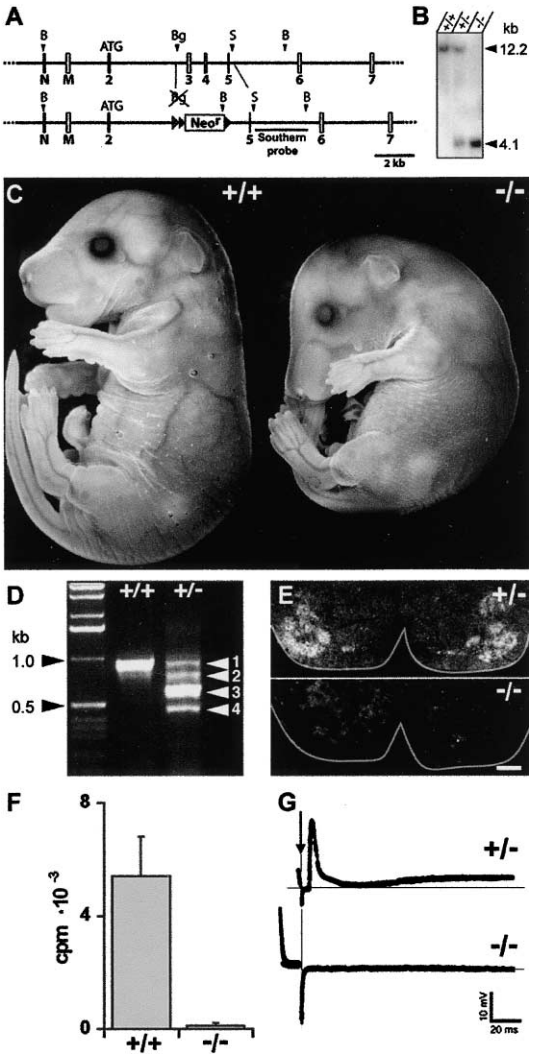

Figure 1. Abolition of Neuromuscular Neurotransmission in *ChAT*$^{-/-}$ Mice

(A) 5′ end of the mouse ChAT gene (top) and targeted allele in which exons 3 and 4 have been replaced with a frt-flanked (black triangles) neomycin-resistance gene (Neo^r; bottom). Gray triangle shows loxP site remaining after excision of exons 3 and 4. B, BamHI; Bg, BglII; S, SpeI; N, M, 5′ noncoding exons.

(B) Confirmation of homologous recombination by Southern analysis from indicated genotypes with probe shown in (A). The BamHI digestion product shifts from 12.2 kb in the wild-type to 4.1 kb in the mutant.

(C) E17 mutant and littermate mice, showing normal gross morphology but hunched posture in mutants.

(D) RT-PCR from brain using primers in exons 2 and 8. Product #1 is the wild-type transcript. Products #2–#4, generated only from the mutant allele, encode truncated fragments of <32 amino acids. Multiple bands reflect heterogeneity downstream of exon 5.

(E) Spinal cord sections stained with anti-ChAT. Motoneurons in the ventral horn (outlined) are immunoreactive in controls but not mutants. Scale bar, 100 μm.

(F) Assay for choline acetylating activity in E19 brain. ChAT activity is readily detectable in control but not mutant extracts. Bars show mean ± SEM, n = 4.

(G) Intracellular recordings from muscle fibers at E19 show that endplate potentials are evoked by nerve stimulation in controls but not mutants. Ends of stimulus artifacts are marked by arrow.

Early Development of Nerve and Muscle

To ask how neuromuscular synapses develop in the absence of synaptic transmission, we initially examined the diaphragm, because synaptogenesis has been well studied in this muscle (reviewed in Greer et al., 1999). In wild-type diaphragm, the first myotubes begin forming on E12 as the first axons reach the muscle. By E13, the phrenic nerve has divided into branches that run along the center of the muscle perpendicular to the myotubes (Figure 2A). By E13.5, axons have left the branches to contact myotubes, and AChR clusters have begun to form. Over the next several days, synapses enlarge and mature (reviewed in Sanes and Lichtman, 1999, 2001). As detailed below, motor axons reach muscles and initiate synapse formation in *ChAT*$^{-/-}$ embryos. Nonetheless, even at the earliest stage examined (E13.0), mutants and controls differed from each other.

Muscle

Muscles were thinner in *ChAT*$^{-/-}$ mice than in littermate controls by E13.5, a difference that became more pronounced over the next several days (Figures 2B–2D). By E16, the liver had herniated through the tendinous center of the diaphragm in most *ChAT*$^{-/-}$ embryos (Figure 2E; >85% of E16–19 mutant embryos but no controls), presumably as a consequence of impaired muscle development (Greer et al., 2000).

We considered three potential explanations for the muscle dysgenesis. First, acetylcholine might promote myogenesis, as suggested by studies in vitro (Entwistle et al., 1988; Krause et al., 1995). Consistent with this possibility, there were fewer fibers in *ChAT*$^{-/-}$ diaphragms than in controls even at E13.5 (Figure 2B). Second, activity might be required for myotube survival, consistent with the known vulnerability of newly formed myotubes to denervation (Sandri and Carraro, 1999). In fact, degenerating, actin-positive myotubes were interspersed with viable myotubes in mutant muscles at E17.5 (Figure 2F). These myotubes had differentiated extensively before dying, as some contained sarcomeres and bore neuromuscular junctions (data not shown). Third, activity might support myotube growth, as expected from the atrophy that occurs following paralysis of postnatal muscle. Consistent with this possibility, the diameter of myotubes was smaller in mutant than in control muscle (Figure 2G). Together, these results imply that neurotransmission plays important roles in promoting muscle formation, maintenance, and/or growth.

Previous papers have described neuromuscular defects in mice lacking agrin or the muscle specific kinase (MuSK), components of the signaling pathway that organizes postsynaptic differentiation (Gautam et al., 1996; DeChiara et al., 1996). NMJs are grossly abnormal in both mutants, and no movement is seen, but motor nerves are present within the muscle, and unclustered AChRs are present on myotubes. Comparison of ChAT, agrin, and MuSK mutants provided a means of asking whether low levels of AChR activation that might occur in agrin and MuSK mutants are sufficient to prevent the muscle dysgenesis seen in the absence of acetylcholine. Agrin and MuSK mutant muscles were thicker and contained more myotubes than ChAT mutant muscles. Moreover, little if any necrosis or atrophy and no herniation were visible in the agrin and MuSK-deficient muscles (Figure 2G and data not shown). These results suggest that acetylcholine can exert effects on developing muscle in the absence of well-formed NMJs.

Phrenic Nerve

As early as E13.5, the phrenic nerve of mutant mice was larger in diameter than that of controls, a difference that persisted throughout embryogenesis (Figure 2H and data not shown). Possible explanations included increased number of axons or axon branches, failure of axons to bundle tightly, or excessive nonneural cells or extracellular matrix. We used electron microscopy to distinguish among these alternatives. As shown in Figures 2I and 2J, the overall structure of the phrenic nerve was normal in mutants: individual axons were wrapped by processes of Schwann cells, and the entire cohort of axon-Schwann cell units was sheathed by a perineurium of fibroblastic processes and connective tissue. Moreover, spacing and size of axons in the nerve did not differ markedly between mutants and controls. However, the number of axons in mutant phrenic nerves was over twice that in control nerves (Figure 2K). The number of Schwann cells (identified by association with axons beneath a shared basal lamina) was also increased in mutant nerves (Figure 2L), perhaps reflecting the known mitogenic effect of axons on Schwann cells (Bunge, 1987).

Either of two known effects of paralysis might account for the increase in axon number. First, neuromuscular paralysis leads to a decrease in the naturally occurring death of motoneurons (Oppenheim, 1991; Banks et al., 2001; Terrado et al., 2001), which occurs from E11.5 to E14.5 at the cervical levels from which the phrenic nerve arises (Yamamoto and Henderson, 1999). Second, paralysis leads to axon branching in adult muscle (collateral sprouting; Brown et al., 1981), and this might also occur in the embryonic nerve trunk. To test for branching, we compared the numbers of axons at proximal and distal points in the same nerves. The number of axons did not differ between proximal and distal levels in controls; there was a slight increase distally in mutants, but it was not statistically significant (Figure 2K). To test for increased motoneuron number, we counted spinal motoneurons in lower cervical and upper thoracic segments of the spinal cord, which innervate the diaphragm as well as other muscles analyzed below, triangularis sterni, crus, and intercostals. The number of motoneurons (identified as large, Nissl-rich somata in the motor columns with prominent nuclei and visible nucleoli) was 79% higher in mutants (15.1 $\pm$ 1.6 [S.E.] per section) than in controls (8.4 $\pm$ 1.1; $p < 0.01$ by Student's t test). Together, these results demonstrate that the number of motoneurons is greater in the absence of neurotransmitter than in its presence.

Intramuscular Nerve Branching and Distribution of Postsynaptic Specializations

The phrenic nerve normally splits into three primary trunks as it nears the diaphragm (Figure 2A). The two largest enter the muscle, then turn in opposite directions and run perpendicular to myotubes; the third runs dorsally to innervate the crus. Small groups of axons leave the nerve trunks, branch further, and innervate myotubes. In *ChAT*$^{-/-}$ mice, the main trunks formed, but there was a dramatic excess of secondary branching, resulting in the nerve covering a larger fraction of the muscle's width in mutants than in controls (Figures 3A–3C). Defects were evident as early as E13, soon after axons entered the muscle but before AChR aggregation was detectable (see below). Although the precise branching pattern varies from embryo to embryo within both mutant and control populations, abnormalities were obvious in all mutants examined at all stages of embryogenesis. Interestingly, defects were confined to intramuscular portions of the nerve, supporting the idea that they resulted from faulty nerve-muscle interactions.

To ask whether branching defects are a general consequence of ChAT deficiency, we examined three other muscles: crus, intercostals, and triangularis sterni (Figures 2A and 2D). All three exhibited excessive secondary branching in mutants (Figures 3D and 3E and data not

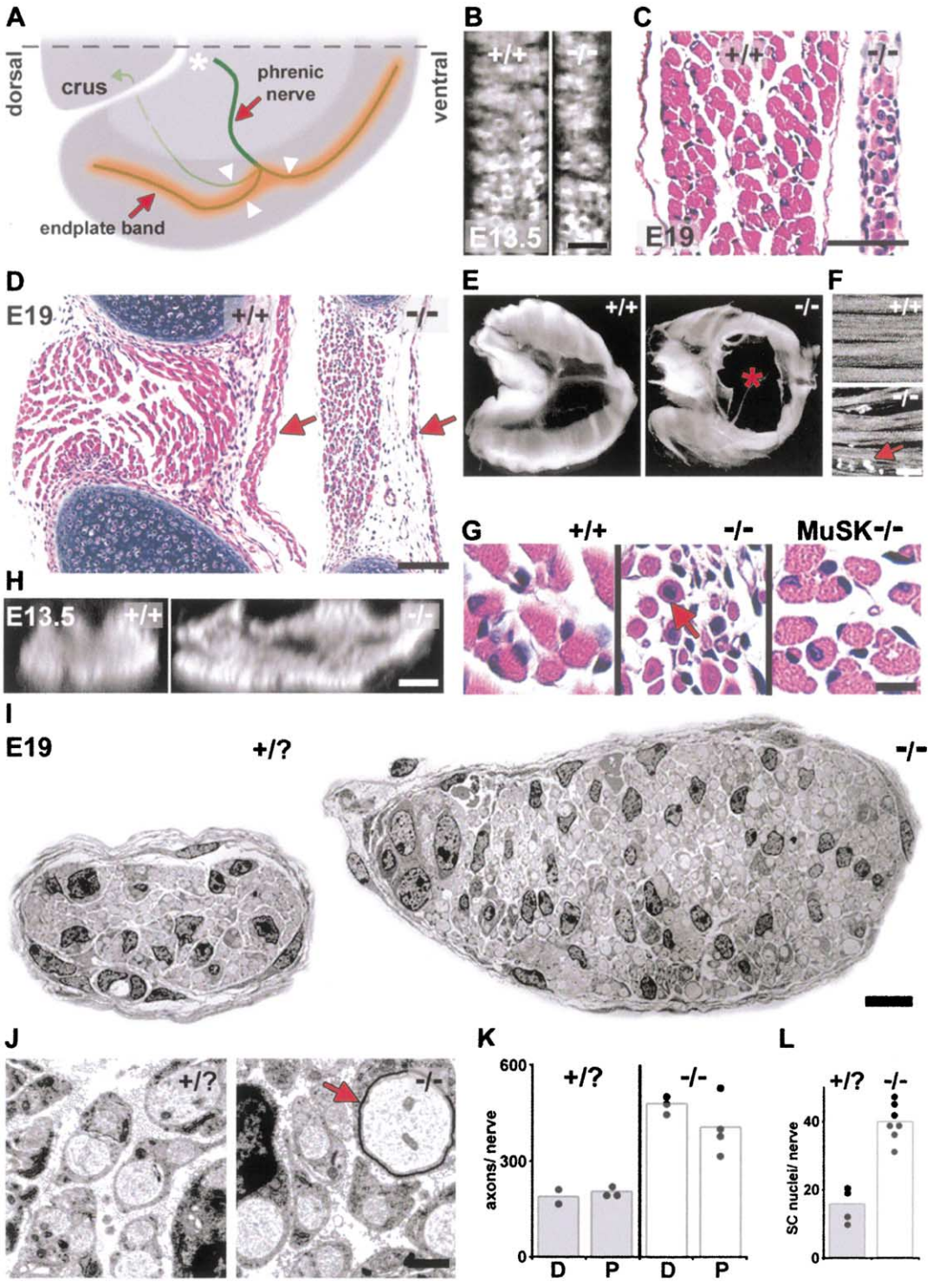

Figure 2. Abnormal Development of Motor Nerves and Muscles in *ChAT*$^{-/-}$ Mice

(A) Sketch of a hemidiaphragm and crus, showing the principal branches of the phrenic nerve (white arrowheads; asterisk, proximal end of phrenic nerve) and the endplate band.

(B and C) Cross-sections of the diaphragm from *ChAT*$^{-/-}$ mice and littermate controls at E13.5 and E19, showing thinner muscles in mutants. (B) is a rotation of a confocal stack from a phalloidin-stained muscle (scale bar, 25 μm); (C) is a haematoxylin-eosin-stained paraffin section (scale bar, 50 μm).

(D) Sections of the intercostals and triangularis sterni (arrows) from E19 mutant and control mice, stained as in (C). Scale bar, 100 μm.

(E) Whole diaphragms at E17, orientated as in (A), showing hernia in mutant (asterisk).

(F) Confocal projection of a phalloidin-stained muscle, showing striations in myotubes of both genotypes but degeneration in the mutant (arrow). Scale bar, 25 μm.

shown). Importantly, intercostals and diaphragm are representative of two different muscle types (FaSyn and DeSyn, respectively) that respond differently to paralysis or denervation in adulthood (Pun et al., 2002). Thus, branching defects are not specific to either of these muscle types, though we cannot exclude the possibility that DeSyn and FaSyn muscles have quantitatively different defects.

The increased branching of intramuscular nerves in the mutants was accompanied by an altered distribution of synapses. Normally, NMJs are confined to a central region, the endplate band, which corresponds to the region in which intramuscular nerves run. To measure the endplate band, we stained AChR clusters in whole mounts with α-bungarotoxin (BTX), drew a polygon connecting the most peripheral synaptic sites, and calculated the average myotube length contained in the polygon (Figure 3F). The endplate band was twice as wide in mutants as in controls in diaphragm, triangularis, and intercostals (Figures 3G and 3H and data not shown).

An obvious possibility was that the endplate band was widened as a consequence of the increased number of motor axons running in the muscle. To test this possibility, we examined mice lacking a proapoptotic protein, BAX. *BAX*$^{-/-}$ mice are viable (Knudson et al., 1995) but show a dramatic decrease in the naturally occurring death of several neuronal populations, including motoneurons (Deckwerth et al., 1996; White et al., 1998). Indeed, phrenic nerves of *BAX*$^{-/-}$ embryos were thickened (data not shown), as documented above for *ChAT*$^{-/-}$ embryos. However, endplate bands of *BAX*$^{-/-}$ diaphragm and triangularis sterni were no wider than those of age-matched controls (Figures 3F–3H). Thus, the influence of neurotransmission on the distribution of synapses in muscle is independent of its role in regulating axon number.

We also asked whether neurotransmission affected the spatial pattern of gene expression in muscle. In normal muscles, the few myonuclei associated with each postsynaptic membrane are transcriptionally specialized; they express genes encoding several components of the postsynaptic membrane, including AChRs, at far higher levels than nonsynaptic myonuclei in the same cytoplasm (Sanes and Lichtman, 1999, 2001). Accordingly, AChR subunit RNAs as well as AChRs are concentrated in endplate bands. Such bands were also present in diaphragm and intercostals muscles from *ChAT*$^{-/-}$ mice. However, endplate bands detected by in situ hybridization, like those detected by BTX staining, were broader and less intense in mutants than in controls (Figures 3I and 3J). Transcriptional specializations were evident in limb as well as axial muscles and were detected from E15 until E18 (data not shown).

An Early Neurotransmitter-Dependent Stage in Postsynaptic Differentiation

For detailed analysis of nascent synapses, we used the triangularis sterni (Figure 2D), because it is only a few fibers thick and, therefore, ideally suited for whole-mount analysis (McArdle et al., 1981). As in diaphragm, AChR aggregates began to form in control triangularis sterni $\sim$E13.5. Initially, most were ovoid and aligned along the long axis of the myotube, but a minority ($<$5%) occurred on slender processes that extended away from the long axis of the myotube (Figures 4A and 4B). Processes were up to 10 μm in length. Possibly similar processes, termed "myopodia," were recently reported to be present in *Drosophila* muscle (Ritzenthaler et al., 2000), and smaller "microprocesses" appear on cultured rodent myotubes (Uhm et al., 2001). We adopt the term "myopodia" although we do not yet know how closely mammalian and fly processes resemble each other. Perhaps myopodia were not described previously in vertebrate muscle because of their rarity and small size or because they are much more difficult to notice in sections than in whole mounts.

AChR clusters appeared on schedule in *ChAT*$^{-/-}$ mutants, but they were smaller than those in controls. Most strikingly, there were $\sim$5-fold more AChR-rich myopodia in mutants than in control (Figure 4A; density of processes $>$5 μm long was 2.27/1000 μm^2 in *ChAT*$^{-/-}$ muscle, 0.47/1000 μm^2 in control muscle, $n = 5$ muscles of each genotype; $p < 0.01$, Mann-Whitney U test). Myopodia were usually in the vicinity of axons, often near varicosities (Figure 4B; $>$50% of myopodia were $<$0.5 μm from an axon—essentially in contact—and only 6% were $>$15 μm from an axon). Some myopodia in mutants were longer and more branched than any seen in controls. These results suggest that the formation or persistence of myopodia is regulated by neurotransmitter. An alternative explanation, that the excessive innervation of *ChAT*$^{-/-}$ myotubes provoked excessive myopodia formation, was ruled out by the observation that few myopodia were present in age-matched *BAX*$^{-/-}$ myotubes (0.50/1000 μm^2), despite their hyperinnervation.

The occurrence of myopodia was transient. In both mutants and controls, AChR-rich patches were oval shaped and flush with the myotube surface by E15–16 (Figure 4D). Mutant postsynaptic sites also acquired other synaptic antigens, such as rapsyn and laminin β2 (Figures 4E and 4F). Thus, by E15–16, the postsynaptic sites on *ChAT*$^{-/-}$ myotubes appeared largely normal by the criteria of size, shape, and molecular architecture.

Differentiation of Nerve Terminals

We next considered the extent to which presynaptic differentiation occurred in the absence of ChAT. In this

(G) Myotubes at E19, stained as in (C), showing decreased diameter and more central nuclei (arrow) in *ChAT*$^{-/-}$ but not in *MuSK*$^{-/-}$ mice. Scale bar, 10 μm.

(H and I) Cross-sections of phrenic nerve at E13.5 ([H], rotation of a confocal stack stained with antibodies to neurofilaments and SV2; scale bar, 5 μm) and E19 ([I], montage of electron micrographs; scale bar, 10 μm), showing increased size of mutant nerve.

(J) Electron micrographs from E19 phrenic nerves, showing Schwann cell-sheathed axons in both genotypes, and some precocious myelination (arrow) in the mutant. Scale bar, 1 μm.

(K and L) Numbers of axons (K) and Schwann cell nuclei (L) in mutant phrenic nerve are approximately double those in control nerves. "D" and "P" signify sections from distal and proximal portions of the nerve (see Results). Bars show means, and dots show individual values. $p <$ 0.01 for differences between all control versus all mutant values in (K) and (L) by Mann-Whitney U test.

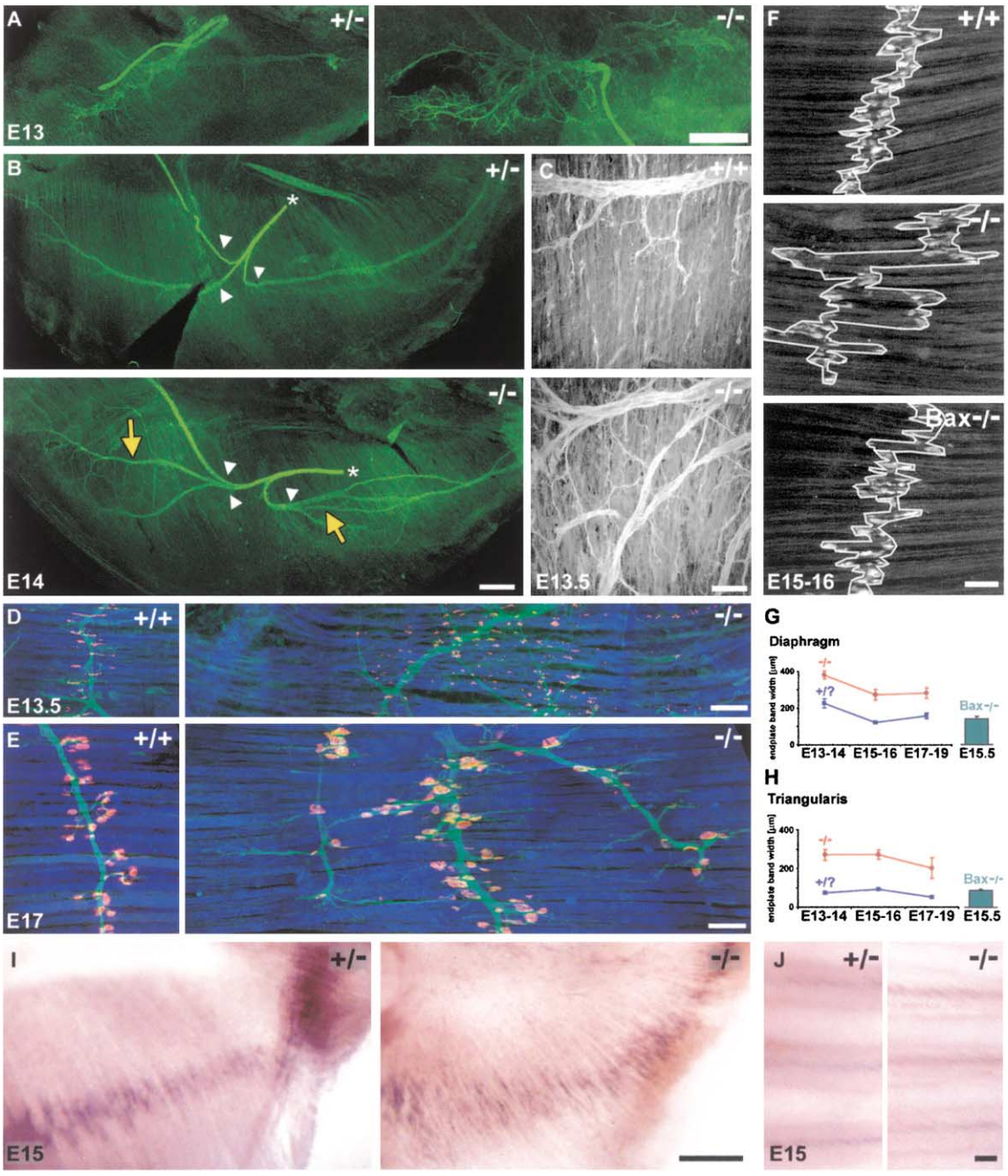

Figure 3. Excessive Nerve Branching and Broad Endplate Bands in *ChAT*$^{-/-}$ but Not *BAX*$^{-/-}$ Muscles

(A–E) Whole mounts of the dorsal quadrant of the diaphragm at E13 (A); hemidiaphragms at E14 (B) and E13.5 (C), and triangularis sterni at E13.5 (D) and E17 (E). In each case, the nerve bears more branches in mutant than in control and covers a larger area of the muscle. In (A)–(C), nerve is stained with anti-neurofilaments and anti-SV2. *, phrenic nerve; arrowheads, main nerve branches (cf. Figure 2A); yellow arrows, additional large branches in mutant. (C) shows higher power views to show excessive secondary branching in the mutant. (D and E) green, anti-neurofilaments and anti-SV2; red, BTX; blue, phalloidin. Scale bar, 250 μm in (A) and (B) and 50 μm in (C)–(E).

(F–H) Width of endplate bands in ChAT and BAX mutants and in controls. (F) shows how measurements were made from BTX-stained whole mounts; for details, see Results. Scale bar, 50 μm. (G) and (H) show measurements from diaphragm and triangularis sterni. Note that the endplate band does not become wider during this period, even though the muscle lengthens by >2-fold. Values are mean ± SEM of 4 to 12 muscles. $p < 0.02$ for differences between *ChAT*$^{-/-}$ and control muscles at each time point in both muscles; $p > 0.2$ for difference between *BAX*$^{-/-}$ muscles and age-matched controls, Mann-Whitney U test.

(I and J) Localization of AChR α subunit RNA, assessed by in situ hybridization at E15. Synapse-associated myonuclei are transcriptionally specialized in mutant and control diaphragm (I) and intercostals (J), but the endplate band is broader and the signal intensity lower in mutants than in controls. Scale bar, 250 μm in (I) and 100 μm in (J).

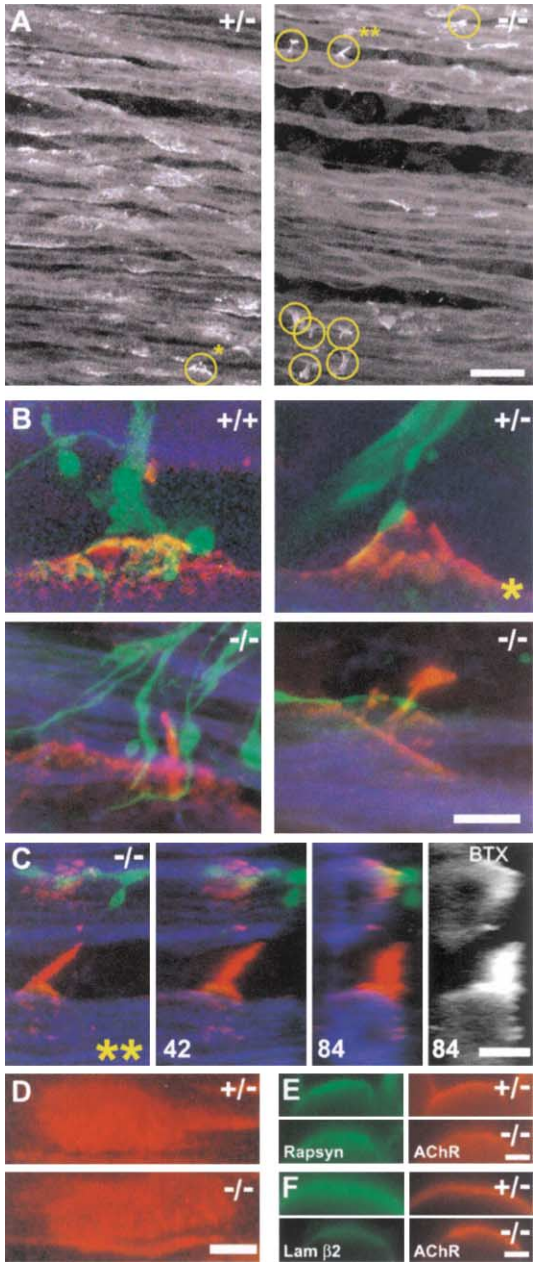

Figure 4. Transient Abundance of AChR-Rich Myopodia in *ChAT*$^{-/-}$ Muscle

(A) E13.5 triangularis sterni stained with BTX. Individual myopodia are circled, and those shown in (B) are marked by * and **. Scale bar, 25 μm. Myopodia are approximately five times more numerous on mutant than on control muscles.

(B) Nerve-muscle appositions from E13.5 muscles such as those in Figure 3C. Many of the AChR-rich (BTX-stained; red) patches of membrane in *ChAT*$^{-/-}$ muscles form "myopodia" that extend perpendicular to the long axis of the myotube (blue). In controls, AChR-rich myopodia are rarer. Most myopodia neighbor varicose-rich terminal branches of motor axons (green). Scale bar, 5 μm.

(C) Confocal reconstruction of a myopodium at E13.5 (staining as in [B]). The image stack is rotated by 42° and 84°. The AChR staining of the 84° rotation is shown in isolation to show that an AChR-patch on the myotube continues onto the myopodium. Scale ar, 5 μm.

(D) By E16, AChR-rich myopodia are rare, and AChR-rich postsynaptic sites are similarly shaped in mutants and controls. Scale bar, 10 μm.

(E and F) Rapsyn (E) and laminin β2 (F) are codistributed with AChRs at both mutant and control synaptic sites. Cross-sections of E17 muscle. Scale bar, 1 μm.

case, abnormalities might reflect not only lack of neurotransmission but also the absence of two major components of the terminal: ChAT itself and the acetylcholine it synthesizes. In several respects, however, nerve terminals formed normally in the absence of their neurotransmitter. Light microscopic examination showed that *ChAT*$^{-/-}$ axons formed synaptic varicosities at NMJs (Figures 4B and 4C). Electron microscopy revealed structurally conventional nerve terminals, closely apposed to the myotube membrane (Figure 5A). The terminals contained numerous electron-lucent synaptic vesicles similar in diameter or abundance to those in control muscles. Moreover, in mutants as in controls, vesicles were concentrated in nerve terminals, with lower density in preterminal portions of the axon. Within nerve terminals, vesicles aggregated near dense regions of the presynaptic membrane, called active zones, where exocytosis occurs (Figure 5B). Active zones were present in similar numbers in mutant and *ChAT*$^{-/-}$ terminals (Figure 5D). Thus, inability to synthesize neurotransmitter does not prevent extensive presynaptic differentiation.

To probe the molecular architecture of synaptic vesicles, we used immunohistochemical methods. Major proteins common to all synaptic vesicles (synaptophysin and SV2), as well as a specific marker of cholinergic vesicles, the vesicular acetylcholine transporter (VAChT; Eiden, 1998), were present in mutant nerve terminals (Figures 5E and 5F and data not shown). Thus, synaptic vesicles acquire generic and at least some transmitter-specific characteristics in the absence of the neurotransmitter itself. Interestingly, ChAT and VAChT genes are in the same genomic locus; the single VAChT coding exon has a polyadenylation signal just 413 bp upstream of the ChAT N exon shown in Figure 1A.

To assay exocytosis from mutant nerve terminals, we treated muscles with the spider venom protein α-latrotoxin (reviewed in Sudhof, 2001). Although its mechanism of action remains incompletely understood, latrotoxin is known to elicit massive transmitter release from adult neuromuscular junctions without detectable effects on preterminal portions of the motor axon. As previously reported for postnatal muscles, latrotoxin depleted vesicles from embryonic control muscles, but active zones persisted (data not shown). Likewise, incubation with latrotoxin but not vehicle led to loss of vesicles from *ChAT*$^{-/-}$ nerve terminals (Figure 5C). This result demonstrates that vesicles lacking both neurotransmitter and neurotransmitter-synthesizing enzyme can nonetheless undergo exocytosis.

Despite the qualitative similarity of control and mutant nerve terminals, they did differ in number and size. Although adult NMJs are singly innervated with a perfect apposition of pre- and postsynaptic elements, developing NMJs are transiently innervated by multiple axons, some of which extend terminal sprouts beyond the confines of the AChR-rich postsynaptic membrane. In mutants, both the number of axons entering individual endplates and the number of axons sprouting beyond

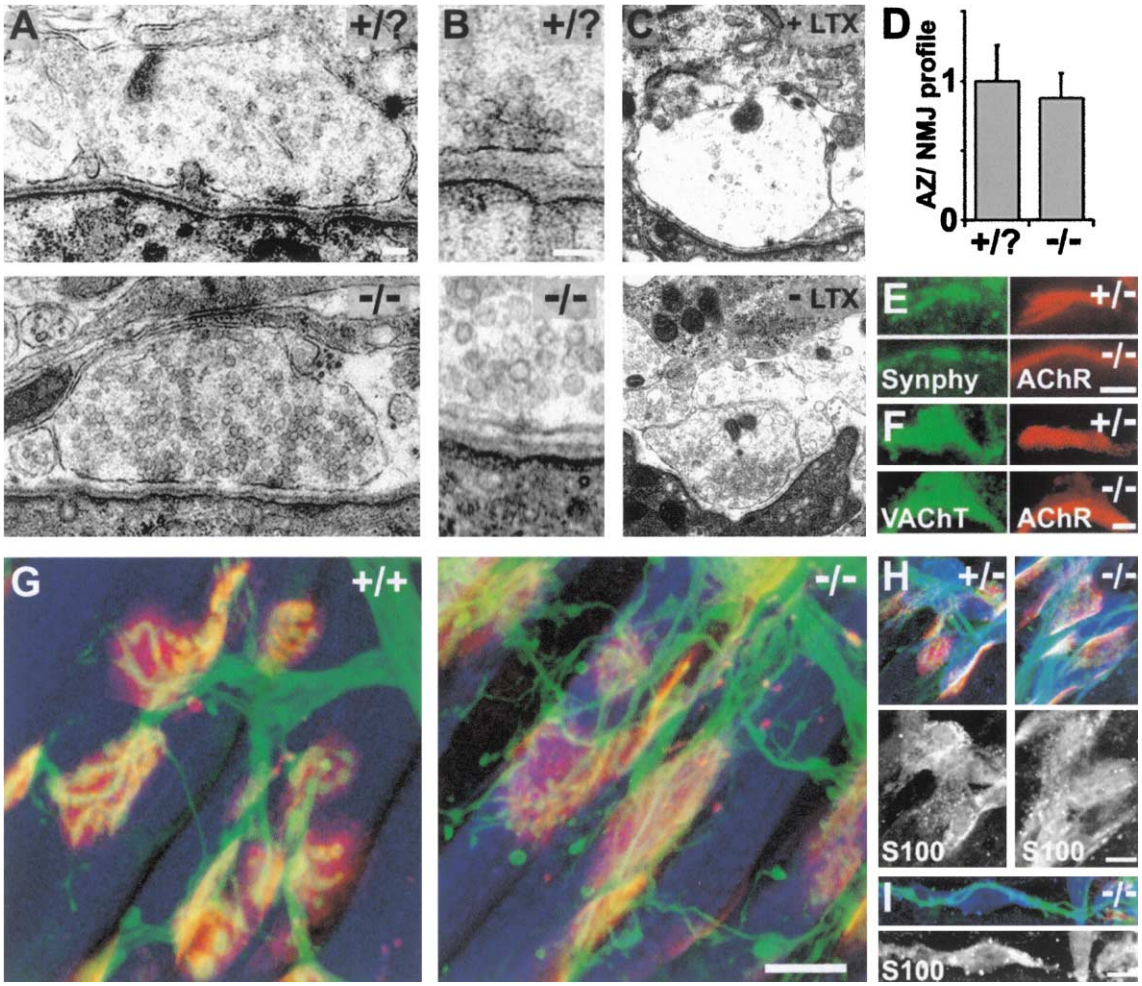

Figure 5. Differentiation of Motor Nerve Terminals that Lack Neurotransmitter

(A and B) Electron micrographs of motor nerve terminals at E18.5. Vesicle-rich terminals are separated from the postsynaptic membrane by a basal lamina and capped by Schwann cell processes. High-magnification views in (B) show vesicles and active zones. Scale bar, 0.15 μm in (A), 0.1 μm in (B).

(C) Electron micrographs of nerve terminals from *ChAT*$^{-/-}$ muscles that were incubated in Ca-free Ringer's solution with (top) or without (bottom) latrotoxin before processing. As in control muscles (data not shown), latrotoxin led to massive exocytosis from *ChAT*$^{-/-}$ nerve terminals, leading to vesicle depletion.

(D) Numbers of active zones in motor nerve terminals, scored in micrographs such as those in panel (A). Bars show mean ± SEM of 13 profiles.

(E and F) Cryostat sections of E17 muscle doubly stained with BTX plus antibodies to a major synaptic vesicle protein, synaptophysin (D), or a component specific to cholinergic synaptic vesicles, VAChT (E). Scale bar, 2.5 μm.

(G) Confocal images of NMJs from E17 whole mounts, showing that motor axons multiply innervate AChR-rich synaptic sites and sprout beyond them, to a greater extent in mutants than in controls. Scale bar, 10 μm.

(H and I) Synaptic sites from muscles stained with anti-S100 (blue and black-and-white panel), NF/SV2 (green), and BTX (red) to show that terminal Schwann cells cap the endplates in mutant as in wild-type animals (H) and that Schwann cells accompany neuronal sprouts in *ChAT*$^{-/-}$ muscles (I). Scale bar, 10 μm.

endplates were increased (Figure 5G; 4.0 ± 0.5 discernible axons entering the junction in mutants versus 2.2 ± 0.2 in controls; 5.4 ± 0.7 sprouts in mutants versus 1.4 ± 0.3 in controls; $p < 0.01$ by Student's t test in both cases).

We also examined Schwann cells, which are closely apposed to nerve terminals at normal NMJs and are known to respond to axon-derived signals. Electron microscopy showed that Schwann cell processes also capped terminals in *ChAT*$^{-/-}$ muscle (Figure 5A and data not shown). Staining for a Schwann cell-specific marker, S-100, showed that the Schwann cells differentiated in the absence of neurotransmission and that the majority of axonal sprouts were associated with Schwann cells (Figures 5H and 5I).

Aberrant Maturation of Synapses

Although NMJs are functional soon after they form, they continue to mature over a prolonged period that lasts until at least the third postnatal week. Many of the later steps in postsynaptic development are thought to be activity dependent (Sanes and Lichtman, 1999). Some

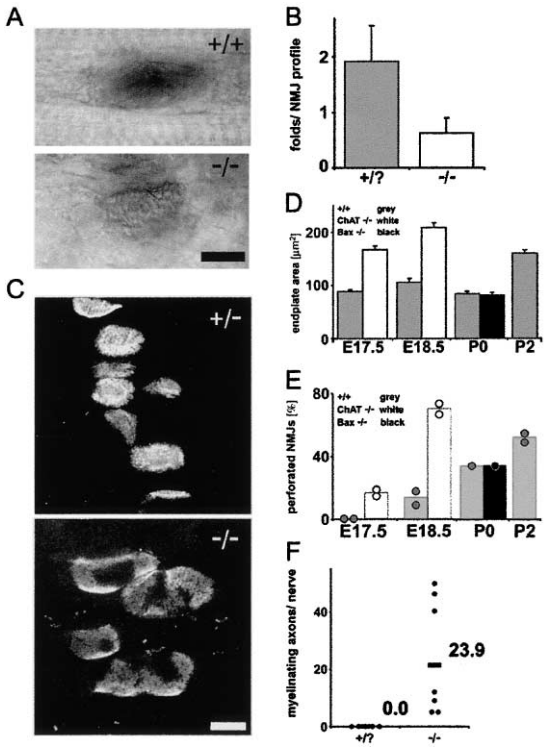

Figure 6. Aberrant Maturation of *ChAT*$^{-/-}$ Neuromuscular Junctions

(A) Cholinesterase activity, detected histochemically in whole mounts at E17. Activity is greater at control than mutant endplates. Scale bar, 10 μm.

(B) Junction folds, scored from electron micrographs such as those in Figure 5C, are more numerous in control than mutant endplates. Bars show mean ± SEM of 13 to 17 profiles.

(C) Precocious growth and perforation of AChR-rich postsynaptic sites. Whole mounts at E19, stained with BTX. Scale bar, 10 μm.

(D and E) Measurements from images such as those in (C). In controls, sites grow perinatally (D), and ovoid plaques become perforated postnatally (E). These aspects of postsynaptic maturation occur precociously in ChAT mutants but not in BAX mutants. Bars in (D) show mean ± SEM from 40 to 80 synapses; $p < 0.001$ for the differences between *ChAT*$^{-/-}$ and control synapses for both time points, Student's t test. Circles in (E) show counts from 40 to 80 synapses in a single muscle.

(F) Number of myelinated axons in the phrenic nerve. Myelination begins postnatally in controls but prenatally in mutants. Each point shows values from one montage, like those in Figures 2I and 2J. Means are indicated. $p < 0.005$ for difference between genotypes, Mann-Whitney U test.

of these steps normally occur during the last days of embryogenesis, allowing us to test their dependence on neurotransmission in *ChAT*$^{-/-}$ mice. For example, levels of synaptic cholinesterase, which normally accumulates after AChRs cluster (Chiu and Sanes, 1984), were lower in mutants than in controls (Figure 6A; 2- to 4-fold difference based on time to reach equivalent staining intensity). This effect was selective, because the density of AChRs was decreased by <20% in mutants at E18.5 (data not shown). Likewise, the number of junctional folds, which begin to invaginate the postsynaptic membrane just before birth, was decreased by ~60% in mutants at E18.5 (Figure 6B).

Postsynaptic maturation was not, however, uniformly delayed in the mutant. The growth of AChR clusters was more rapid in mutants than in controls. Mutant and control clusters were similar in area on E15–16, but the average area in mutants was 89% and 68% larger than that of controls at E17.5 and E19, respectively (Figures 6C and 6D). Even more striking was a change in the shape of the NMJ. In wild-type mice, most AChR clusters are uniform and ovoid at birth; shortly thereafter, the plaque becomes perforated to form a "doughnut," which is the first step in elaboration of the branched "pretzel-shaped" morphology of the adult (Slater, 1982; Marques et al., 2000). In mutant muscles, some plaques were perforated by E17.5, and ~70% were perforated before birth (Figures 6C and 6E). Such precocity was not observed in *BAX*$^{-/-}$ mutants, suggesting that it was not a consequence of neuronal excess (Figures 6D and 6E).

We also noted that the phrenic nerve matured precociously in *ChAT*$^{-/-}$ mice. In controls, myelination occurs exclusively postnatally, but some axons were myelinated in mutants by birth (Figures 2J and 6F).

Number and Spacing of *ChAT*$^{-/-}$ Neuromuscular Junctions

In most mammalian skeletal muscles, including diaphragm and triangularis sterni, muscle fibers bear a single synaptic site. Multiple axons initially innervate that site, then all but one is withdrawn postnatally, by a process called synapse elimination (Sanes and Lichtman, 1999). As noted above, the extent of hyperinnervation is greater in mutants than controls. In addition, confocal imaging of whole mounts revealed that many myotubes in *ChAT*$^{-/-}$ muscles were innervated at multiple sites, each of which bore a specialized postsynaptic membrane (Figures 7A and 7B). The distance between synaptic sites ranged from tens to hundreds of micrometers, and in many cases, their innervation was derived from different nerve branches. These results suggest that activity plays a role in setting the number of NMJs on a muscle fiber.

Because we were concerned that closely apposed myotubes might be difficult to distinguish in whole mounts, we counted the number of AChR clusters >1 μm long on myotubes teased from fixed muscles (Figure 7D). This was equivalent to numbers of NMJs, because confocal images showed that all clusters of >1 μm were innervated at this age. Surprisingly, analysis of teased fibers revealed a low incidence of multiple endplates in controls, which was not appreciated previously (Bennett and Pettigrew, 1974). However, the fraction of myotubes with multiple AChR-rich synaptic sites was 5-fold higher in mutants than in controls (Figure 7C).

Discussion

We studied neuromuscular junctions of *ChAT*$^{-/-}$ mice to learn how synapses form in the absence of their neurotransmitter. The array of phenotypes we observed included (1) increased numbers of axons and Schwann cells in the motor nerve, (2) increased branching of intramuscular nerves from the onset of synaptogenesis, (3) widened endplate zones, (4) widened bands of transcriptionally specialized nuclei, (5) decreased number and size of myotubes, (6) signs of myotube necrosis, (7) profusion of AChR-rich myopodia in the vicinity of nerve

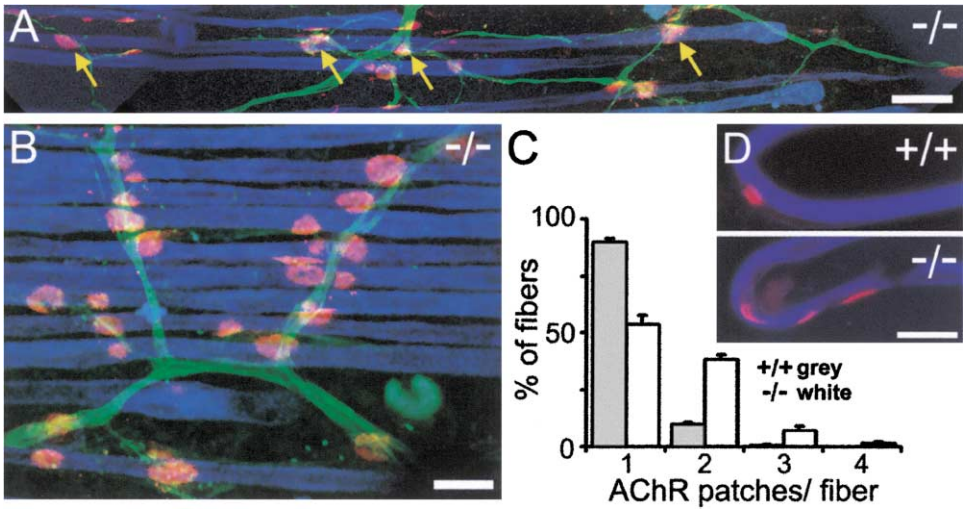

Figure 7. Multiple Synaptic Sites on Individual Myotubes in *ChAT*$^{-/-}$ Mice

(A and B) Whole mounts of *ChAT*$^{-/-}$ triangularis sterni at E18.5 (A) and E17 (B), stained as in Figure 3C. Confocal projections show multiple synapses on individual myotubes. (A) shows four sites on one myotube (arrows), three of which are innervated by axons from a single nerve branch. (B) shows several myotubes with two sites. Each is innervated from a separate nerve branch, leading to a doubled endplate band. Scale bar, 50 μm in (A), 25 μm in (B).

(C and D) Single fibers were teased from BTX-stained triangularis sterni at E17 (D), and the number of AChR-rich sites per myotube was counted on a total of 271 control and 362 mutant myotubes from four muscles of each genotype (C). Note that only a portion of the teased myotube is shown in (D); larger fields were visualized to obtain the counts in (C). Scale bar, 25 μm in (D).

terminals, (8) multiple synaptic sites on individual myotubes, (9) hyperinnervation of individual synaptic sites, (10) AChR-rich sites that are initially smaller but eventually larger than those in age-matched controls, (11) decreased levels of acetylcholinesterase in the synaptic cleft, (12) decreased numbers of junctional folds in the postsynaptic membrane, (13) precocious appearance of perforations in AChR-rich aggregates, and (14) precocious myelination of motor axons. Some of these results confirm those of previous studies, but others reveal unexpected roles of neurotransmission in synaptogenesis.

The altered numbers of motor axons and myotubes in *ChAT*$^{-/-}$ mice are consistent with previous demonstrations that paralysis of chick and rodent embryos leads to decreased motoneuron death and muscular dysgenesis (Harris, 1981a; Ding et al., 1983; Oppenheim, et al., 1989; Houenou et al., 1990; Oppenheim, 1991; Banks et al., 2001; Terrado et al., 2001). In the present context, the most important implication of these results is that some synaptic defects may be consequences of the abnormal "landscape" in which the synapses form. Indeed, we initially suspected that the broadened distribution of synapses in the mutant might be a consequence of the increased number of motor axons. Analysis of BAX mutants, in which naturally occurring motoneuron death is greatly reduced (Deckwerth et al., 1996; White et al., 1998), showed that this was not the case. BAX mutants also allowed us to exclude the possibility that proliferation of myopodia and precocious postsynaptic differentiation, discussed below, were indirect consequences of increased motoneuron numbers.

How might inactivity regulate synaptic distribution? One possibility is that the width of the endplate band is determined by the muscle and then refined by the nerve. This interpretation is suggested by the finding that AChR clusters and transcriptionally specialized nuclei in aneural muscle form in abnormally broad central bands (Yang et al., 2001; Lin et al., 2001) similar to those seen in *ChAT*$^{-/-}$ muscle. Thus, the neurotransmitter might be the neural influence that refines the "prepattern" to decrease the size of a zone that axons recognize as susceptible to innervation. Alternatively, the broader endplate band in the ChAT mutants might reflect the overproduction of muscle-derived axonal growth factors that are normally downregulated by activity (Oppenheim, 1991; Sanes and Lichtman, 1999). Similar alternatives apply to the multiple synaptic sites on individual myotubes: activity might decrease the area over which individual myotubes are susceptible to innervation (Gordon et al., 1974; see Skorpen et al., 1999, for discussion), or a retrograde influence from inactive muscle might stimulate axons to grow new synaptic branches.

Neurotransmission affects the structure as well as the distribution of synaptic contacts: there are ~5-fold more AChR-rich myopodia in mutants than in controls. Myopodia have been implicated in synaptogenesis in *Drosophila* muscle (Ritzenthaler et al., 2000), and smaller but possibly related processes were recently reported to be present in cultured rodent myotubes (Uhm et al., 2001). Interestingly, Uhm et al. (2001) showed that microprocesses were most prominent in regions of apposition to axons and that their number was increased by bath application of agrin, a nerve-derived organizer of postsynaptic differentiation (Burgess et al., 1999; Sanes and Lichtman, 2001). These results, along with our observation that myopodia number and size are increased in *ChAT* mutants, suggest that nerves use both agrin and acetylcholine to shape their postsynaptic target; agrin might stimulate formation of myopodia, and neurotransmission might lead to their disassembly. In this way, an

ingrowing axon could attract its postsynaptic partner, then stabilize a contact once a functional synapse is established. Analysis of agrin/ChAT double mutants may provide a way to test this hypothesis. Interestingly, myopodia resemble in some respects the dendritic filopodia that have been implicated as active partners in the formation of central synapses (Ziv and Smith, 1996; Wong et al., 2000).

Together, these alterations in numbers of axons, axonal branches, myotubes, and myopodia challenge the widely held view that early aspects of synaptogenesis are activity independent (see Introduction and Goodman and Shatz, 1993, for references). In vitro, motor axons can release neurotransmitter even before they contact myotubes and activate AChRs almost immediately upon contact (Hume et al., 1983; Chow and Poo, 1985). Our results strongly suggest that such release is developmentally important. Moreover, neurons exhibit spontaneous activity even before they form synapses, and, at least in vitro, activity can affect early events such as neuronal differentiation and axonal outgrowth (reviewed in Zhang and Poo, 2001; Spitzer, 2002). Thus, so many early events relevant to synaptogenesis are activity dependent that, in a very real sense, synaptogenesis itself is regulated by activity from its inception. A distinction between activity-independent and -dependent phases may be valid for simplified preparations, such as dissociated, cultured neurons, but cannot be extended to the embryo.

At later stages, some aspects of synaptic maturation were delayed in the mutant, but other aspects occurred precociously. Levels of synaptic AChE and numbers of junctional folds were decreased, consistent with previous results (Gordon et al., 1974; Lomo and Slater, 1980; Betz et al., 1980; Rubin et al., 1980; Duxson, 1982; Michel et al., 1994; Washbourne et al., 2002). Indeed, AChE expression is regulated by nerve-evoked activity. However, AChR-rich synaptic areas grew faster and acquired a perforated appearance *earlier* in mutants than in controls. The annular appearance of plaques seen in mutant embryos resembles an intermediate step in the transformation of plaques into branch-shaped NMJs in postnatal normal mice (Slater, 1982; Marques et al., 2000). Such precocity may point to the existence of a homeostatic signaling system of the sort that has been proposed to act at *Drosophila* NMJs (DiAntonio et al., 1999) and in cultured rodent neurons (Turrigiano and Nelson, 2000; Murthy et al., 2001). In these systems, decreased postsynaptic activity leads to an increase in synaptic size or efficacy. By analogy, inactivity might lead the muscle to increase the size of its receptive surface. The hyperinnervation and precocious myelination we observe might also be parts of a homeostatic system; these aspects would likely require the existence of a retrograde signal by which muscle promotes presynaptic maturation in inverse proportion to its level of activity. Indeed, such a system has been invoked to explain the effects of activity on motoneuron number (see above) and the observation that adult muscles accept innervation when denervated but are refactory to hyperinnervation when already innervated (Jansen et al., 1973). In any event, the outcome is that the inactive synapse is neither globally retarded nor precocious but has elements of both and is therefore aberrant.

Finally, we note some limitations of our study. First, as mentioned above, the multiplicity of abnormalities makes it difficult to determine which effects of inactivity are primary and which are consequences of earlier defects. A second limitation is that acetylcholine may be involved in more than conventional neuromuscular transmission even at the NMJ. For example, Schwann cells respond to acetylcholine (Georgiou et al., 1999), so lack of ChAT might affect their development, which might, in turn, affect other aspects of synaptogenesis. Third, autonomic and central cholinergic synapses are surely affected in the mutant, and even some nonneuronal cells bear cholinergic receptors, but neonatal lethality makes these structures difficult to study. Indeed, preliminary observations have revealed dermal abnormalities in mutants (T.M., unpublished data), consistent with suggestions that keratinocytes are cholinergically regulated (Grando, 1997). Fourth, some roles of synaptic activity are likely to be based on *differences* in activity between axons rather than the total amount of activity in the circuit, in which case complete blockade of activity may not be informative. Fortunately, the allele we generated is conditional, so we may be able to circumvent some of these limitations. In the studies presented here, ChAT exons were deleted in germ cells, so the mutants were nulls. In the future, however, we can deliver cre under temporal or spatial control, to excise ChAT after synaptogenesis is underway or in just a subset of motoneurons. In addition, limiting excision to supraspinal portions of the nervous system may allow us to bypass lethality and study central cholinergic pathways.

Conclusions

From the multiplicity of abnormalities observed in *ChAT*$^{-/-}$ mutants, we draw the following main conclusions. (1) Neurotransmission regulates the numbers of all three synaptic components: motor axons, myotubes, and Schwann cells. Thus, in addition to effects on synaptogenesis per se, activity profoundly affects the landscape in which synapses form. (2) Neurotransmission affects the number and distribution of synaptic sites and the number of axons at a single site. As shown by the *BAX*$^{-/-}$ mutant, at least some of these effects are independent of the increase in axon number and therefore likely to indicate a more direct effect of activity on innervation pattern. (3) Some nascent postsynaptic sites are on transient myopodia that appear to "reach out" to terminal varicosities. Their number is increased in mutants, indicating an early role for activity in forming or stabilizing nerve-muscle contacts. (4) Nerve terminals can differentiate extensively in the absence of their neurotransmitter. (5) Some aspects of synaptic development are delayed in the absence of neurotransmission, but others occur precociously. Thus, neurotransmission is better viewed as coordinating rather than promoting synaptic maturation.

Experimental Procedures

Mutant Mice

A targeting vector was constructed from a bacterial artificial chromosome (Genome Systems) containing the ChAT locus. First, a 12.2 kb BamHI fragment was subcloned into pBluescript. A SpeI/BamHI fragment was deleted from the 3′ end, leaving a 9.6 kb BamHI/SpeI

fragment. A loxP site with synthetic Sau3A ends was amplified by PCR and cloned into a unique BglII site 700 bp upstream of exon 3 (numbered as in Misawa et al., 1992). Subsequently, a cassette containing a second loxP site and a TN5 Neo gene flanked by Frt sites was introduced 200 bp downstream of exon 4 by homologous recombination in bacteria (Zhang et al., 1998). In this way, exons 3 and 4 were flanked by loxP sites. Two copies of a thymidine kinase gene were inserted at the NotI site of pBluescript for negative selection in ES cells. The construct was electroporated into ES cells, homologous recombinants were obtained, and one clone was injected into blastocysts to generate germline chimeras and then heterozygotes. For the studies reported here, the heterozygotes were bred to a Beta actin-Cre transgenic line (Lewandoski and Martin, 1997) to delete exons 3 and 4 and generate null mutants.

For studies of agrin, we used the null allele generated in our laboratory by R.W. Burgess (Lin et al., 2001). MuSK (DeChiara et al., 1996) and BAX (Knudson et al., 1995) mutants have been described previously. *MuSK*$^{+/-}$ mice were obtained from T. DeChiara and G. Yancopoulos (Regeneron Pharmaceuticals), and *BAX*$^{+/-}$ mice were obtained from Girish Putcha and E. Johnson (Washington University).

Biochemical and Molecular Biological Assays

Genotypes of ChAT mutants were determined by PCR on tail DNA, using separate pairs of primers for the wild-type allele (CAACCGCC TGGCCCTGCCAGTCAACTCTAG and GAGGATGAAATCCTGACA GATTCCAACAGG) and for the mutant allele (TGGTTCTTTCCGCC TCAGGACTCTTCCTTT and TAACCAAACGTAATATATGTTTGTTG GAGC). Transcripts from the ChAT gene were examined by RT-PCR. Whole heads were homogenized in Trizol solution (Gibco). Five micrograms of total RNA from each sample was reverse transcribed using the Superscript II kit (Invitrogen) according to the manufacturer's protocol, except that a mix of random hexamers and oligo dT primers was used. PCR was performed under standard conditions with the following primers: exon 2, GTCGGCAGCTCTGCTACTC TGG; exon 8, CGCTCCATTCAAGCTGCAGCCTC; exon 15, GCTGA CTCCTGTCGGACATTGGC. Reaction products were separated by agarose gel electrophoresis, purified from the gel (Qiagen), and sequenced.

ChAT activity was assayed in Triton extracts of whole brain by the radiometric method of Fonnum (1975).

Histology

For light microscopic examination of whole mounts, embryos were decapitated and their thoraci fixed by submersion in 4% paraformaldehyde for several days. The muscles of interest were then dissected out and stained overnight with murine monoclonal antibodies against neurofilaments (SMI32; Sternberger) and SV-2 (Developmental Studies Hybridoma Bank) in saline containing 5% normal goat serum, 2% bovine serum albumin, and 0.2% Triton X-100. Following extensive washing, the muscles were incubated with secondary antibody (Cy2-conjugated donkey-anti-mouse Ig; Jackson), plus Alexa594-labeled BTX (Molecular Probes) to stain AChRs, and Alexa660-labeled phalloidin (Molecular Probes) to label actin. Confocal images were obtained on a Biorad 1024 confocal laser scanning microscope equipped with a Krypton-Argon-Laser mounted on an Olympus BX50 microscope using a 10× objective (air, N.A. 0.3) for overview montages, a 40× objective (oil, N.A.1.35 or water, N.A.1.15) for intermediate, and a 100× objective (oil, N.A. 1.4) for high-magnification images. Images were processed with Metamorph software (Universal Imaging) and edited in Photoshop (Adobe).

To study the molecular architecture of the NMJ, we fixed muscles for 30–60 min in 4% paraformaldehyde, then froze the tissue and cut sections in a cryostat. Sections were stained as above, using goat anti-ChAT (Chemicon), goat anti-VAChT (Promega), mouse anti-SV2 (Developmental Studies Hybridoma Bank), rabbit anti-synaptophysin (Zymed), rabbit anti-rapsyn (made in our laboratory), or rabbit anti-laminin-β2 (gift of R. Timpl). To visualize cholinesterase, we used the histochemical method of Karnovsky and Roots (1964).

Tissue for electron microscopy was fixed in 4% glutaraldehyde plus 4% paraformaldehyde, refixed in osmium tetroxide, and embedded in resin. Thin sections were stained with uranyl acetate and lead citrate. Active zones and junctional folds were quantified as described in Patton et al. (2001). In some cases, muscles were dissected and were treated for 20 min at 37°C with 1 μM α-latrotoxin (Sigma) in Ca-free mouse Ringer's solution (119 mM NaCl, 2.5 mM KCl, 3.3 mM $MgCl_2$, 1 mM NaH_2PO_4, 11 mM glucose, 20 mM Hepes, 1 mM EGTA) before fixation for electron microscopy. Controls were kept in Ca-free Ringer's without toxin.

In situ hybridization was performed on whole mounts as in Lin et al. (2001) using digoxygenin-labeled probes. The AChR-α riboprobes were generated from PCR fragments amplified from exon 9 of the AChR-α gene (5′ primer CGTGAGGAATGGAAGTATG, 3′ primer AAC AACTAGCCATGGCAATAC). Viral promoters were added to the primers to permit in vitro transcription from the PCR product.

Electrophysiology

Ribcages from E18.5 mice were perfused (1–2 ml/min) with oxygenated Dulbecco's modified Eagle's medium (4 mM calcium) at room temperature. Intercostal muscle fibers were impaled under a dissecting microscope with 3 M KCl-filled glass electrodes, and the corresponding nerve was stimulated through a suction electrode. Potentials were recorded using a microprobe-system (M701, WPI). For field stimulation of muscle, the tip of the suction electrode was placed directly onto the muscle surface.

Acknowledgments

We thank Sarah Bird and Mia Wallace for assistance; and Dr. Stephen Eglen for statistical advice. This work was supported by grants from the National Institutes of Health to J.W.L. and J.R.S. and by a fellowship from the Emmy-Noether-Program of the Deutsche Forschungsgemeinschaft to T.M.

Received: June 25, 2002
Revised: September 19, 2002

References

Akaaboune, M., Culican, S.M., Turney, S.G., and Lichtman, J.W. (1999). Rapid and reversible effects of activity on acetylcholine receptor density at the neuromuscular junction in vivo. Science *286*, 503–507.

Banks, G.B., Chau, T.N., Bartlett, S.E., and Noakes, P.G. (2001). Promotion of motoneuron survival and branching in rapsyn-deficient mice. J. Comp. Neurol. *429*, 156–165.

Bennett, M.R., and Pettigrew, A.G. (1974). The formation of synapses in striated muscle during development. J. Physiol. *241*, 515–545.

Betz, H., Bourgeois, J.P., and Changeux, J.P. (1980). Evolution of cholinergic proteins in developing slow and fast skeletal muscles in chick embryo. J. Physiol. *302*, 197–218.

Broadie, K., and Bate, M. (1993). Activity-dependent development of the neuromuscular synapse during Drosophila embryogenesis. Neuron *11*, 607–619.

Brown, M.C., Holland, R.L., and Hopkins, W.G. (1981). Motor nerve sprouting. Annu. Rev. Neurosci. *4*, 17–42.

Bunge, R.P. (1987). Tissue culture observations relevant to the study of axon-Schwann cell interactions during peripheral nerve development and repair. J. Exp. Biol. *132*, 21–34.

Burgess, R.W., Nguyen, Q.T., Son, Y.J., Lichtman, J.W., and Sanes, J.R. (1999). Alternatively spliced isoforms of nerve- and muscle-derived agrin: their roles at the neuromuscular junction. Neuron *23*, 33–44.

Carbini, L.A., and Hersh, L.B. (1993). Functional analysis of conserved histidines in choline acetyltransferase by site-directed mutagenesis. J. Neurochem. *61*, 247–253.

Chiu, A.Y., and Sanes, J.R. (1984). Development of basal lamina in synaptic and extrasynaptic portions of embryonic rat muscle. Dev. Biol. *103*, 456–467.

Chow, I., and Poo, M.M. (1985). Release of acetylcholine from embryonic neurons upon contact with muscle cell. J. Neurosci. *5*, 1076–1082.

Dahm, L.M., and Landmesser, L.T. (1991). The regulation of synapto-

genesis during normal development and following activity blockade. J. Neurosci. *11*, 238–255.

DeChiara, T.M., Bowen, D.C., Valenzuela, D.M., Simmons, M.V., Poueymirou, W.T., Thomas, S., Kinetz, E., Compton, D.L., Rojas, E., Park, J.S., et al. (l996). The receptor tyrosine kinase MuSK is required for neuromuscular junction formation in vivo. Cell *85*, 501–512.

Deckwerth, T.L., Elliott, J.L., Knudson, C.M., Johnson, E.M., Jr., Snider, W.D., and Korsmeyer, S.J. (1996). BAX is required for neuronal death after trophic factor deprivation and during development. Neuron *17*, 401–411.

Deitcher, D.L., Ueda, A., Stewart, B.A., Burgess, R.W., Kidokoro, Y., and Schwarz, T.L. (1998). Distinct requirements for evoked and spontaneous release of neurotransmitter are revealed by mutations in the Drosophila gene neuronal-synaptobrevin. J. Neurosci. *18*, 2028–2039.

DiAntonio, A., Petersen, S.A., Heckmann, M., and Goodman, C.S. (1999). Glutamate receptor expression regulates quantal size and quantal content at the Drosophila neuromuscular junction. J. Neurosci. *19*, 3023–3032.

Ding, R., Jansen, J.K., Laing, N.G., and Tonnesen, H. (1983). The innervation of skeletal muscles in chickens curarized during early development. J. Neurocytol. *12*, 887–919.

Duxson, M.J. (1982). The effect of postsynaptic block on development of the neuromuscular junction in postnatal rats. J. Neurocytol. *11*, 395–408.

Eiden, L.E. (1998). The cholinergic gene locus. J. Neurochem. *70*, 2227–2240.

Entwistle, A., Zalin, R.J., Warner, A.E., and Bevan, S. (1988). A role for acetylcholine receptors in the fusion of chick myoblasts. J. Cell Biol. *106*, 1703–1712.

Featherstone, D.E., Rushton, E., and Broadie, K. (2002). Developmental regulation of glutamate receptor field size by nonvesicular glutamate release. Nat. Neurosci. *5*, 141–146.

Fonnum, F. (1975). A rapid radiochemical method for the determination of choline acetyltransferase. J. Neurochem. *24*, 407–409.

Gautam, M., Noakes, P.G., Mudd, J., Nichol, M., Chu, G.C., Sanes, J.R., and Merlie, J.P. (1995). Failure of postsynaptic specialization to develop at neuromuscular junctions of rapsyn-deficient mice. Nature *377*, 232–236.

Gautam, M., Noakes, P.G., Moscoso, L., Rupp, F., Scheller, R.H., Merlie, J.P., and Sanes, J.R. (1996). Defective neuromuscular synaptogenesis in agrin-deficient mutant mice. Cell *85*, 525–535.

Georgiou, J., Robitaille, R., and Charlton, M.P. (1999). Muscarinic control of cytoskeleton in perisynaptic glia. J. Neurosci. *19*, 3836–3846.

Goodman, C.S., and Shatz, C.J. (1993). Developmental mechanisms that generate precise patterns of neuronal connectivity. Cell *72*, 77–98.

Gordon, T., Perry, R., Tuffery, A.R., and Vrbova, G.G. (1974). Possible mechanisms determining synapse formation in developing skeletal muscles of the chick. Cell Tissue Res. *155*, 13–25.

Grando, S.A. (1997). Biological functions of keratinocyte cholinergic receptors. J. Investig. Dermatol. Symp. Proc. *2*, 41–48.

Greer, J.J., Allan, D.W., Martin-Caraballo, M., and Lemke, R.P. (1999). An overview of phrenic nerve and diaphragm muscle development in the perinatal rat. J. Appl. Physiol. *86*, 779–786.

Greer, J.J., Allan, D.W., Babiuk, R.P., and Lemke, R.P. (2000). Recent advances in understanding the pathogenesis of nitrofen-induced congenital diaphragmatic hernia. Pediatr. Pulmonol. *29*, 394–399.

Harris, A.J. (1981a). Embryonic growth and innervation of rat skeletal muscles. I. Neural regulation of muscle fibre numbers. Philos. Trans. R. Soc. Lond. B Biol. Sci. *293*, 257–277.

Harris, A.J. (1981b). Embryonic growth and innervation of rat skeletal muscles. III. Neural regulation of junctional and extra-junctional acetylcholine receptor clusters. Philos. Trans. R. Soc. Lond. B Biol. Sci. *293*, 287–314.

Houenou, L.J., Pincon-Raymond, M., Garcia, L., Harris, A.J., and Rieger, F. (1990). Neuromuscular development following tetrodotoxin-induced inactivity in mouse embryos. J. Neurobiol. *21*, 1249–1261.

Hume, R.I., Role, L.W., and Fischbach, G.D. (1983). Acetylcholine release from growth cones detected with patches of acetylcholine receptor rich membranes. Nature *305*, 632–634.

Jansen, J.K., Lomo, T., Nicolaysen, K., and Westgaard, R.H. (1973). Hyperinnervation of skeletal muscle fibers: dependence on muscle activity. Science *181*, 559–561.

Karnovsky, M.J., and Roots, L. (1964). A "direct-coloring" thiocholine method for holinesterases. J. Histochem. Cytochem. *12*, 219–221.

Knudson, C.M., Tung, K.S., Tourtellotte, W.G., Brown, G.A., and Korsmeyer, S.J. (1995). Bax-deficient mice with lymphoid hyperplasia and male germ cell death. Science *270*, 96–99.

Krause, R.M., Hamann, M., Bader, C.R., Liu, J.H., Baroffio, A., and Bernheim, L. (1995). Activation of nicotinic acetylcholine receptors increases the rate of fusion of cultured human myoblasts. J. Physiol. *489*, 779–790.

Lewandoski, M., and Martin, G.R. (1997). Cre-mediated chromosome loss in mice. Nat. Genet. *17*, 223–225.

Lin, W., Burgess, R.W., Dominguez, B., Pfaff, S.L., Sanes, J.R., and Lee, K.F. (2001). Distinct roles of nerve and muscle in postsynaptic differentiation of the neuromuscular synapse. Nature *410*, 1057–1064.

Lomo, T., and Slater, C.R. (1980). Control of junctional acetylcholinesterase by neural and muscular influences in the rat. J. Physiol. *303*, 191–202.

Marques, M.J., Conchello, J.A., and Lichtman, J.W. (2000). From plaque to pretzel: fold formation and acetylcholine receptor loss at the developing neuromuscular junction. J. Neurosci. *20*, 3663–3675.

McArdle, J.J., Angaut-Petit, D., Mallart, A., Bournaud, R., Faille, L., and Brigant, J.L. (1981). Advantages of the triangularis sterni muscle of the mouse for investigations of synaptic phenomena. J. Neurosci. Methods *4*, 109–115.

Michel, R.N., Vu, C.Q., Tetzlaff, W., and Jasmin, B.J. (1994). Neural regulation of acetylcholinesterase mRNAs at mammalian neuromuscular synapses. J. Cell Biol. *127*, 1061–1069.

Misawa, H., Ishii, K., and Deguchi, T. (1992). Gene expression of mouse choline acetyltransferase: Alternative splicing and identification of a highly active promoter region. J. Biol. Chem. *267*, 20392–20399.

Murthy, V.N., Schikorski, T., Stevens, C.F., and Zhu, Y. (2001). Inactivity produces increases in neurotransmitter release and synapse size. Neuron *32*, 673–682.

Oppenheim, R.W. (1991). Cell death during development of the nervous system. Annu. Rev. Neurosci. *14*, 453–501.

Oppenheim, R.W., Bursztajn, S., and Prevette, D. (1989). Cell death of motoneurons in the chick embryo spinal cord. XI. Acetylcholine receptors and synaptogenesis in skeletal muscle following the reduction of motoneuron death by neuromuscular blockade. Development *107*, 331–341.

Parsons, R.L., Calupca, M.A., Merriam, L.A., and Prior, C. (1999). Empty synaptic vesicules recycle and undergo exocytosis at vesamicol-treated motor nerve terminals. J. Neurophysiol. *81*, 2696–2700.

Patton, B.L., Cunningham, J.M., Thyboll, J., Kortesmaa, J., Westerblad, H., Edstrom, L., Tryggvason, K., and Sanes, J.R. (2001). Properly formed but improperly localized synaptic specializations in the absence of laminin α4. Nat. Neurosci. *4*, 597–604.

Pun, S., Sigrist, M., Santos, A.F., Ruegg, M.A., Sanes, J.R., Jessell, T.M., Arber, S., and Caroni, P. (2002). An intrinsic distinction in neuromuscular junction assembly and maintenance in different skeletal muscles. Neuron *34*, 357–370.

Ritzenthaler, S., Suzuki, E., and Chiba, A. (2000). Postsynaptic filopodia in muscle cells interact with innervating motoneuron axons. Nat. Neurosci. *3*, 1012–1017.

Rubin, L.L., Schuetze, S.M., Weill, C.L., and Fischbach, G.D. (1980). Regulation of acetylcholinesterase appearance at neuromuscular junctions in vitro. Nature *283*, 264–267.

Saitoe, M., Schwarz, T.L., Umbach, J.A., Gundersen, C.B., and Kido-

koro, Y. (2001). Absence of junctional glutamate receptor clusters in Drosophila mutants lacking spontaneous transmitter release. Science *293*, 514–517.

Sandri, M., and Carraro, U. (1999). Apoptosis of skeletal muscles during development and disease. Int. J. Biochem. Cell Biol. *31*, 1373–1390.

Sanes, J.R., and Lichtman, J.W. (1999). Development of the vertebrate neuromuscular junction. Annu. Rev. Neurosci. *22*, 389–442.

Sanes, J.R., and Lichtman, J.W. (2001). Induction, assembly, maturation and maintenance of a postsynaptic apparatus. Nat. Rev. Neurosci. *2*, 791–805.

Sepich, D.S., Wegner, J., O'Shea, S., and Westerfield, M. (1998). An altered intron inhibits synthesis of the acetylcholine receptor α-subunit in the paralyzed zebrafish mutant nic1. Genetics *148*, 361–372.

Skorpen, J., Lafond-Benestad, S., and Lomo, T. (1999). Regulation of the size and distribution of ectopic neuromuscular junctions in adult skeletal muscle by nerve-derived trophic factor and electrical muscle activity. Mol. Cell. Neurosci. *13*, 192–206.

Slater, C.R. (1982). Postnatal maturation of nerve-muscle junctions in hindlimb muscles of the mouse. Dev. Biol. *94*, 11–22.

Spitzer, N.C. (2002). Activity-dependent neuronal differentiation prior to synapse formation: the functions of calcium transients. J. Physiol. (Paris) *96*, 73–80.

Sudhof, T.C. (2001). α-Latrotoxin and its receptors: neurexins and CIRL/latrophilins. Annu. Rev. Neurosci. *24*, 933–962.

Sweeney, S., Broadie, K., Keane, J., Niemann, H., and O'Kane, C. (1995). Targeted expression of tetanus toxin light chain in *Drosophila* specifically eliminates synaptic transmission and causes behavioral defects. Neuron *14*, 341–351.

Terrado, J., Burgess, R.W., DeChiara, T., Yancopoulos, G., Sanes, J.R., and Kato, A.C. (2001). Motoneuron survival is enhanced in the absence of neuromuscular junction formation in embryos. J. Neurosci. *21*, 3144–3150.

Turrigiano, G.G., and Nelson, S.B. (2000). Hebb and homeostasis in neuronal plasticity. Curr. Opin. Neurobiol. *10*, 358–364.

Uhm, C.S., Neuhuber, B., Lowe, B., Crocker, V., and Daniels, M.P. (2001). Synapse forming axons and recombinant agrin induce microprocess formation on myotubes. J. Neurosci. *21*, 9678–9689.

Varoqueaux, F., Sigler, A., Rhee, J.S., Brose, N., Enk, C., Reim, K., and Rosenmund, C. (2002). Total arrest of spontaneous and evoked synaptic transmission but normal synaptogenesis in the absence of Munc13-mediated vesicle priming. Proc. Natl. Acad. Sci. USA *99*, 9037–9042.

Verhage, M., Maia, A.S., Plomp, J.J., Brussaard, A.B., Heeroma, J.H., Vermeer, H., Toonen, R.F., Hammer, R.E., van den Berg, T.K., Missler, M., et al. (2000). Synaptic assembly of the brain in the absence of neurotransmitter secretion. Science *287*, 864–869.

Washbourne, P., Thompson, P.M., Carta, M., Costa, E.T., Mathews, J.R., Lopez-Bendito, G., Molnar, Z., Becher, M.W., Valenzuela, C.F., Partridge, L.D., et al. (2002). Genetic ablation of the t-SNARE SNAP-25 distinguishes mechanisms of neuroexocytosis. Nat. Neurosci. *5*, 19–26.

White, F.A., Keller-Peck, C.R., Knudson, C.M., Korsmeyer, S.J., and Snider, W.D. (1998). Widespread elimination of naturally occurring neuronal death in Bax-deficient mice. J. Neurosci. *18*, 1428–1439.

Wong, W.T., Faulkner-Jones, B.E., Sanes, J.R., and Wong, R.O. (2000). Rapid dendritic remodeling in the developing retina: dependence on neurotransmission and reciprocal regulation by Rac and Rho. J. Neurosci. *20*, 5024–5036.

Yamamoto, Y., and Henderson, C.E. (1999). Patterns of programmed cell death in populations of developing spinal motoneurons in chicken, mouse, and rat. Dev. Biol. *214*, 60–71.

Yang, X., Arber, S., William, C., Li, L., Tanabe, Y., Jessell, T.M., Birchmeier, C., and Burden, S.J. (2001). Patterning of muscle acetylcholine receptor gene expression in the absence of motor innervation. Neuron *30*, 399–410.

Zhang, L.I., and Poo, M.M. (2001). Electrical activity and development of neural circuits. Nat. Neurosci. *4*, 1207–1214.

Zhang, Y., Buchholz, F., Muyrers, J.P., and Stewart, A.F. (1998). A new logic for DNA engineering using recombination in Escherichia coli. Nat. Genet. *20*, 123–128.

Ziv, N.E., and Smith, S.J. (1996). Evidence for a role of dendritic filopodia in synaptogenesis and spine formation. Neuron *17*, 91–102.